Dynamic characterization of electrodynamic bearings combined with active magnetic dampers

Qingwen CUI*, Fabrizio IMPINNA**, Lester D. SUAREZ CABRERA**, Joaquim G. DETONI**, Nicola AMATI**, Andrea TONOLI** and Hannes BLEULER*

*Laboratory of Robotic Systems (LSRO), Ecole Polytechnique Federale de Lausanne.
ME D3 1016, Station 9, CH–1015 Lausanne, Switzerland
E-mail: qingwen.cui@epfl.ch
**Mechatronics Lab., Department of Mechanical and Aerospace Engineering, Politecnico di Torino
Corso Duca deghi Abruzzi 24, 10129, Torino, Italy

Abstract

Electrodynamic Bearings (EDBs) are a kind of passive magnetic bearings that exploits the interaction between the eddy currents in a rotating conductor and the stationary magnetic field to provide restoring forces. They have been regarded as an appealing alternative to Active Magnetic Bearings (AMBs), having the possibility to obtain stable levitation using standard conductive materials at room temperature without introducing negative stiffness in any direction. Compared to AMBs, EDBs present advantages such as lower cost, higher reliability due to simplicity of configurations. However, applications of EDBs are still limited due to instability issues. The rotating damping force arising in EDBs causes unstable behavior of the rotor, which requires a stabilizing solution. A hybrid solution is presented in the present paper, where Active Magnetic Dampers (AMDs) are applied to provide non-rotating damping to the rotor supported by EDBs to obtain stable operation. This solution is designed to exploit the high reliability of EDBs, overcoming the stability problem by means of controllable AMDs. Rather than using active electromagnetic actuators to provide stiffness (like in standard AMBs), the AMBs here are used as dampers only (thus called AMDs), resulting in downsized and more efficient AMBs. The effect of the EDB−AMD system has been studied both analytically and experimentally. A dedicated test rig has been built to validate the analytical model and to characterize the system. Dynamic characterization of the system is presented, demonstrating the effectiveness of this solution and dynamics of the system.

Keywords : Electrodynamic bearing, Magnetic bearing, Active magnetic damper, Hybrid magnetic bearing, Stability of electrodynamic bearing, Rotordynamic stability

1. Introduction

Magnetic bearings are attractive devices especially for high speed operation because of their capability of providing contactless levitation for rotors. Active magnetic bearings (AMBs) are the classical magnetic bearings that have been under research for years and they have reached the level of industrial applications. However, AMBs are costly and complicated due to power electronics and control units, although the controllability of rotordynamics in AMB systems is indeed an advantage.

Electrodynamic bearings (EDBs), as one kind of passive magnetic bearing, have been regarded as an appealing alternative, having the ability to provide positive stiffness passively without introducing negative stiffness in any direction (Detoni, 2013). EDBs provide restoring force on the rotor exploiting the interaction between the induced eddy currents in the rotating conductor and the static magnetic field. They are characterized with the possibility to obtain stable levitation using standard conductive materials at room temperature, requiring no control systems, power electronics or sensors. Despite promising characteristics of EDBs, rotors supported by EDBs are subject to different types of instabilities. The main issue is that the effect of the rotating damping force in EDBs causes unstable behavior of the rotor. Two main solutions based on passive systems have been proposed in literature. Filatov et al. (2006) presented a solution with eddy current dampers to introduce non-rotating damping to the rotor. Tonoli et al. (2011) proposed to introduce an elastic and dissipative element between the statoric part of the bearing and the base of the machine. Although stable levitation is possible, the effectiveness of the existing methods is still limited (Detoni, et al., 2014). These solutions do not allow fully levitating the rotor at low rotating speeds. Besides, the amount of damping could only be modified during the design phase. These issues limit the applications of EDBs and require more efforts to find an optimal solution.

A hybrid solution has been proposed by the authors (Impinna, et al., 2014), where EDBs are combined with active magnetic dampers (AMDs). In this configuration, AMB systems are introduced together with EDBs in order to provide non-rotating damping to the rotor instead of acting as bearings. Thus the system will be called EDB–AMD system. This system is designed to exploit the high reliability of EDBs overcoming the stability problem by means of controllable AMDs. It results in increased global system reliability. In case of AMBs failure, the EDBs are able to guarantee a stable levitation down to a certain speed considered safe for touch-down. It also allows investigation on the dynamics and damping strategies of EDBs.

In the present paper, the combination of electrodynamic and AMD forces is studied both analytically and experimentally. An analytical model of the system is obtained by coupling a 4 degrees of freedom rotor model together with EDBs and AMD models. A dedicated test rig has been built to validate the analytical model and to characterize the system. Simulations and experimental tests are exploited for the validation and the characterization.

2. Test rig of the EDB–AMD system

The configuration of the EDB–AMD system is shown in Fig. 1a. It consists of two radial EDB units with two AMDs and one axial-flux electric motor at the center of the rotor, based on the EDB system designed in (Amati, et al., 2012) with AMDs added. The axial degree of freedom is controlled passively, using the magnetic flux closure of AMDs as reluctance bearing. The goal of this test-rig (Fig.1) is to demonstrate the performance of the proposed hybrid magnetic bearing system and to validate the analytical model. The main parameters of the test rig are given in Table 1.

(a)

(b)

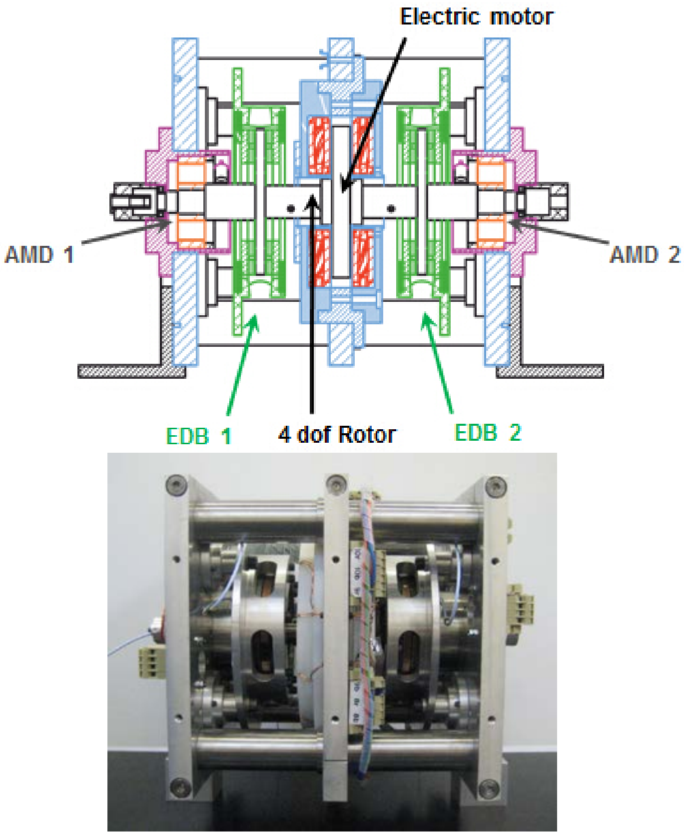

Fig. 1 (a) Configuration of the EDB–AMD system, (b) the test rig

Table 1 Parameters of the test rig.

Parameter	Description	Value
ω	Nominal speed	20000 rpm
m_r	Rotor mass	4.35 kg
l_r	Rotor length	305 mm
J_p	Polar moment of inertia	0.00572 kg·m^2
J_t	Transversal moment of inertia	0.01995 kg·m^2

The EDBs in this test rig have a double flux homopolar configuration to improve stiffness and minimize the power losses. The configuration is shown in Fig. 2a. Each EDB is composed of four ring shaped permanent magnets magnetized axially and bonded to two back iron discs (with two magnet rings on each back iron disc). The magnets are oriented in attraction so that the flux lines are closed as shown in Fig. 2b. The geometric parameters of the double flux EDB from the design procedure are listed in Table 2.

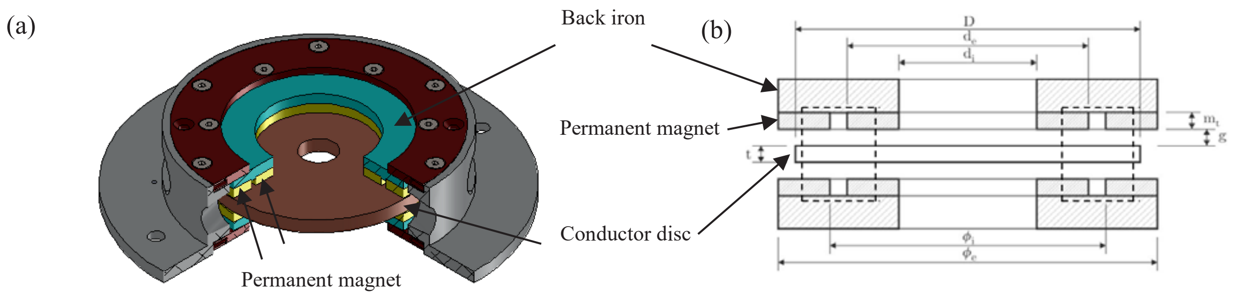

Fig. 2 (a) Configuration of the double flux EDB, (b) cross section view of the EDB

Table 2 Geometric parameters of the double flux EDB.

Parameter	Description	Value
D	Conductor outer diameter	120 mm
de	Inner permanent magnet outer diameter	89 mm
di	Inner permanent magnet inner diameter	64 mm
mt	Permanent magnet thickness	5.5 mm
t	Conductor disc thickness	8 mm
g	Axial air gap	0.75 mm
Φ_e	Outer permanent magnet outer diameter	120 mm
Φ_t	Outer permanent magnet outer diameter	95 mm

In this test rig, the AMDs can be used as active magnetic bearings to guarantee suspension for speeds below the EDB's stability threshold or for speeds where EDBs are not able to provide sufficient levitation forces. The AMDs act as pure damper for higher speeds ensuring a stable levitation over a wide speed range. A PID architecture is used in the position control of AMDs to provide proper stiffness and damping. With properly tuned control parameters of the AMDs, the rotor is able to levitate and rotate within a stable speed range of 0 to 6000 rpm. Experimental tests have been conducted within this speed range. The AMD actuators are classical 8-pole planar actuators. The configuration is shown in Fig.3. Some geometric parameters of the actuators are listed in Table 3.

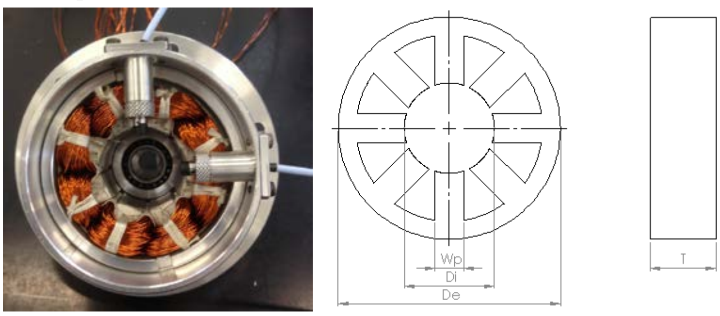

Fig. 3 Configuration of the 8-pole actuator

Table 3 Geometric parameters of the AMDs.

Parameter	Description	Value
D_e	Outer diameter	152 mm
D_i	Inner diameter	31 mm
W_p	Pole width	10 mm
T	Actuator thickness	22.5 mm
N	Number of turns	53
W_d	Wire diameter	0.63 mm

3. Modeling of the EDB–AMD system

The analytical model of the EDB–AMD rotor system has been established. It consists of a 4 degrees of freedom model of the rotor supported by the combination of electrodynamic suspension and AMDs. Thus it includes three main parts: rotor, EDB and AMD. Analytical models of the subsystems are built and then coupled together. The model is crucial to study the rotordynamic stability and to determine the control strategies for the AMD actuators in the speed range. The block diagram of the system is shown in Fig.4. Considering a reference frame where the *z*–axis represents the axial coordinate and the *x, y*–axes are the fixed radial coordinates, the rotor receives the forces in *x* and *y* directions by the EDBs and AMDs. The outputs of the rotor are the radial positions of the shaft referring to the EDBs and AMDs positions. The EDBs generate radial forces in function of the displacements and the rotating speed as inputs to the whole system. No axial force is produced by the EDBs. The AMDs react to the radial positions from the sensors and generate a force proportional to the first derivative of the position error thus adding non–rotating damping to the system. The system's performance is modeled with Simulink® for simulations.

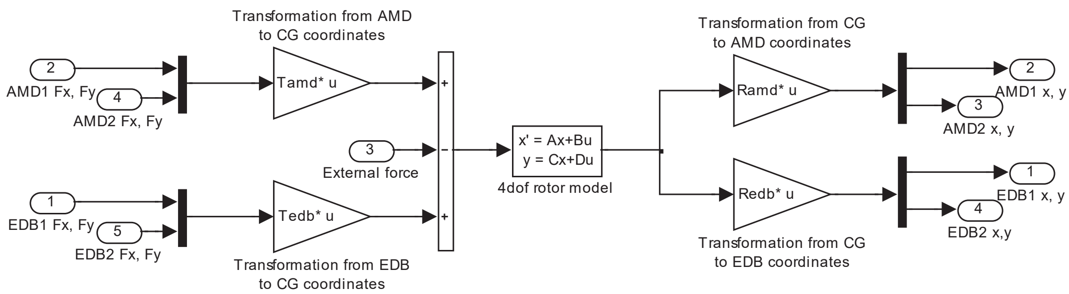

Fig. 4 Block diagram of the system in Simulink

The analytical model of the 4 dof rotor supported on EDBs refers to the work of Detoni, et al. (2014). Models of the EDB and AMD are presented in the following sections.

3.1 EDB model

The modeling of electrodynamic bearings is thoroughly explained in (Amati, et al., 2008). The Lorentz force generated by the eddy currents in the conductor can be modeled as two orthogonal branches in the rotating frame $\eta\xi$ (Fig. 5a). Each branch is composed by the series connection of a linear spring and a viscous damper. The EDB force generated by the double flux configuration can be represented with two parallel sets of spring and damper (Fig. 5b). Therefore the double flux EDB is characterized by the parameters k_1, c_1, k_2 and c_2 instead of k and c. Parameters of the mechanical equivalent for the double flux EDB are shown in Table 4.

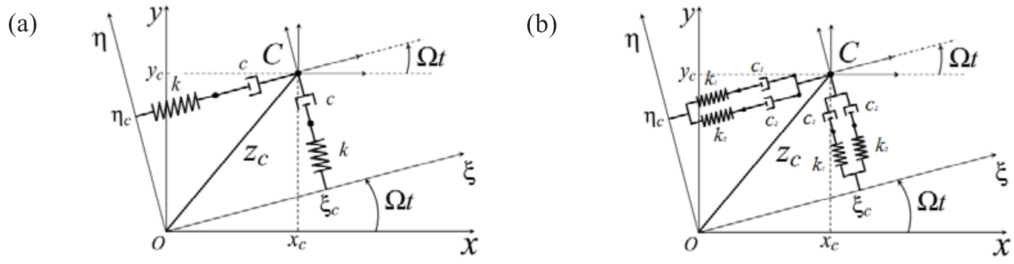

Fig. 5 Mechanical equivalent of EDBs. (a) single flux configuration, (b) double flux configuration.

Table 4 Parameters of the double flux EDB mechanical equivalent.

Parameter	Description	Value
ω_{EDB}	EDB electric pole	5000 rpm
k_1	EDB equivalent stiffness1	200010N/m
k_2	EDB equivalent stiffness2	123979 N/m
c_1	EDB equivalent damping1	57.7 Ns/m
c_2	EDB equivalent damping2	349.8 Ns/m

The corresponding dynamic equations of motion written in the State Space format are:

$$\begin{Bmatrix} \dot{x}_{EDB} \\ \dot{y}_{EDB} \\ \dot{F}_{x1EDB} \\ \dot{F}_{y1EDB} \\ \dot{F}_{x2EDB} \\ \dot{F}_{y2EDB} \end{Bmatrix} = \begin{bmatrix} 0 & 0 & 0 & 0 & 0 & 0 \\ 0 & 0 & 0 & 0 & 0 & 0 \\ 0 & k_1\Omega & -\omega_{RL1} & -\Omega & 0 & 0 \\ -k_1\Omega & 0 & \Omega & -\omega_{RL1} & 0 & 0 \\ 0 & k_2\Omega & 0 & 0 & -\omega_{RL2} & -\Omega \\ -k_2\Omega & 0 & 0 & 0 & \Omega & -\omega_{RL2} \end{bmatrix} \begin{Bmatrix} x_{EDB} \\ y_{EDB} \\ F_{x1EDB} \\ F_{y1EDB} \\ F_{x2EDB} \\ F_{y2EDB} \end{Bmatrix} + \begin{bmatrix} 1 & 0 \\ 0 & 1 \\ k_1 & 0 \\ 0 & k_1 \\ k_2 & 0 \\ 0 & k_2 \end{bmatrix} \begin{Bmatrix} \dot{x}_{EDB} \\ \dot{y}_{EDB} \end{Bmatrix} \tag{1}$$

where the suffix *EDB* indicates that the forces and displacements are referred to the plane of action of the EDB. The terms $\omega_{RL1}=k_1/c_1$ and $\omega_{RL2}=k_2/c_2$ are the poles of the two electric circuits arising in the rotating conductor (Amati, et al., 2012).

3.2 AMD model

The force of an electromagnetic actuator at the operation point can be linearized as (Schweitzer, et al., 2009):

$$f_x(\mathrm{x},\mathrm{i}) = k_i i + k_x x \tag{2}$$

where k_x and k_i are respectively the negative displacement stiffness and the current stiffness of the actuator. Therefore the linearized equations of the AMD actuators in the fixed x and y directions are:

$$\begin{Bmatrix} F_x \\ F_y \end{Bmatrix} = \begin{bmatrix} k_x & 0 \\ 0 & k_x \end{bmatrix} \begin{Bmatrix} x_{AMD} \\ y_{AMD} \end{Bmatrix} + \begin{bmatrix} k_i & 0 \\ 0 & k_i \end{bmatrix} \begin{Bmatrix} i_{Cx} \\ i_{Cy} \end{Bmatrix} \tag{3}$$

The variables x_{AMD}, i_{Cx}, y_{AMD} and i_{Cy} indicate respectively the displacements and the control currents in the two directions x and y of the actuator action plane. The numerical values of the AMD stiffnesses are obtained analytically (Table 5).

Table 5 Parameters of AMDs..

Parameter	Description	Value
k_x	Displacement stiffness	-20 N/mm
k_i	Current stiffness	9.5 N/A
K_p	Controller proportional gain	10 A/mm
T_d	Derivative time constant	0.005 s
T_i	Integral time	0.1 s
N	Time constant of the first order derivative filter	5 s

A PID architecture is used in the position control of AMDs to provide proper stiffness and damping. The transfer function between position error and reference control currents in each direction of the AMD is:

$$\frac{i_{c\_AMD}}{\varepsilon_{\_AMD}} = K_p\left(1+\frac{1}{T_i \cdot s}+\frac{T_d \cdot s}{1+\frac{T_d}{N}\cdot s}\right) \tag{4}$$

where s is the Laplace variable. All the controller parameters are listed in Table 5. PID control is used just for quasi-static characterization, where the integral term is needed to keep the rotor at a reference position. While for the rest tests of the EDB–AMD system, PD control is used, because the EDBs will not provide levitation force if the rotor is centered. The corresponding non-rotating damping c_n can be obtained with the following equation:

$$c_n = K_p \cdot T_d \cdot k_i \tag{5}$$

3. Dynamic characterization

3.1 Model validation

In this section the analytical model of the EDB–AMD rotor system will be validated both with quasi–static tests and frequency response measurements.

Quasi-static characterization is commonly used in the field of EDB identification, where the rotor is fixed in an off-centered radial position and rotates at a certain speed. In the test rig, the rotor rotates with a fixed eccentricity, which is kept by PID control of the AMDs. The EDBs produce restoring forces due to the eccentricity, whereas the AMDs are required to provide the same amount of forces with opposite directions to keep the rotor in the off–centered position. Thus the values of EDB forces are obtained by measuring the AMD forces, which can be calculated from the measured control currents. With an eccentricity of 0.1 mm in $+y$ direction, the control currents in AMDs are measured experimentally in the speed range of 0 to 6000 rpm. The corresponding AMD forces are calculated. Consequently the values of EDB forces are obtained, which are plotted in Fig. 6a to be compared with analytical results. The force comparison well validates the model.

To illustrate the dynamic performance of the system, measurements of frequency responses are carried out experimentally as well as with simulations. A reference current is given along one of the axes x_1, y_1, x_2, and y_2 of the two AMDs, the corresponding frequency response of displacements in the same direction is measured with a frequency sweep from 10 to 500 Hz. The transfer function between input current and output displacement in one axis is obtained with the rotor levitated and static (Ω=0). The comparison of analytical and experimental results is shown in Fig. 6b, which shows good agreement.

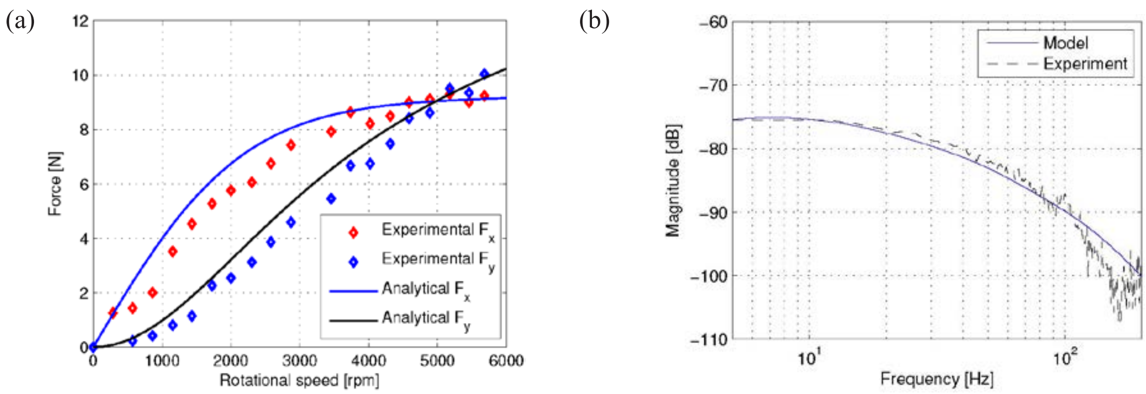

Fig. 6 (a) EDB force comparison according to rotational speed, (b) frequency response plot with input current and output displacement in x_1 direction.

3.2. Damping analysis

Stability analysis of the system is investigated to understand the amount of non-rotating damping required to keep the rotor in stable operation. Simulations with the validated model are used in this analysis. Figure 7 illustrates the minimum amount of non-rotating damping required from one of the AMD actuators to keep the rotor stable for different speeds. It can be noted that this plot shows similar fashion with the rotating damping developed in the EDB. The required damping value increases according to the rotational speed up to its maxima, which occurs around the electric pole of the EDBs. The maximum amount of non–rotating damping required for the rotor's stable operation is 371 Ns/m. This curve characterizes the damping demand in the EDB system and can be used to define the control parameters in the AMD. Besides, the curve could be also useful to find an alternative solution of stabilizing EDB systems.

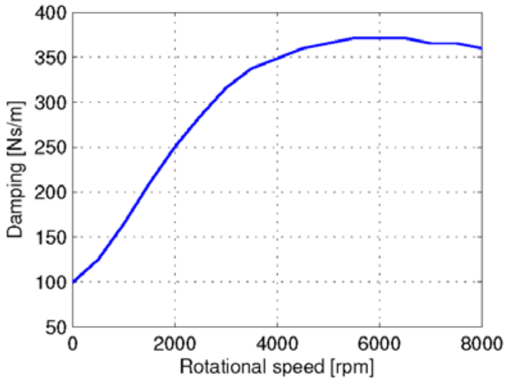

Fig. 7 Minimum value of non-rotating damping required from each AMD actuator according to rotational speed.

3.3. Control currents and power consumption

The AMD control currents i_{Cx} and i_{Cy} according to the rotating speed using PID control and PD control are plotted respectively in Fig. 8. With PID control, the levitation is mainly provided by AMDs. They work as pure AMBs since the rotor is kept centered by the actuators. Thus the control currents remain almost constant in the speed range. While using PD control of the AMDs, the rotor is not kept centered by the actuators. The restoring force is provided by EDBs. At low speed, the control currents are even higher compared to the case with PID control, which is due to the fact that with eccentricity there is the contribution of negative displacement stiffness. Thus more control currents are required to compensate the effect of the negative stiffness. With the rotational speed increasing, the contribution of EDB restoring force increases consequently. The eccentricity is getting smaller. The load on AMDs is also reduced, so that the AMD control currents reduce according to the rotating speed. The difference in evolutions of i_{Cx} and i_{Cy} is also due to the effect of EDB forces, which have different behaviors in the directions parallel and perpendicular to the eccentricity as shown in Fig. 6a. Therefore, at high operation speed, the amount of control currents in the actuator is significantly smaller compared to standard AMB system.

Consequently, the total power consumption in the EDB–AMD system can be presented. The power consumption in the EDB could be obtained with the product of torque and angular speed, whereas the power consumption in AMDs is calculated directly with the obtained currents in the coils and the electrical resistances. This calculation does not include eddy current or windage losses in the actuators since they are relatively small in general. The total consumed power due to EDBs and AMDs in the system are plotted in Fig. 8b. The AMB power consumption is obtained by using PID position control of the actuators. It can be noticed that, the power consumption in EDBs is rather small compared to that in AMDs. At low speed, AMDs consume more power compared to standard AMBs, which is due to the effect of negative displacement stiffness in the actuators as explained in the previous section. At high speed, the sum of power consumption in EDBs and AMDs can be reduced significantly compared to AMBs.

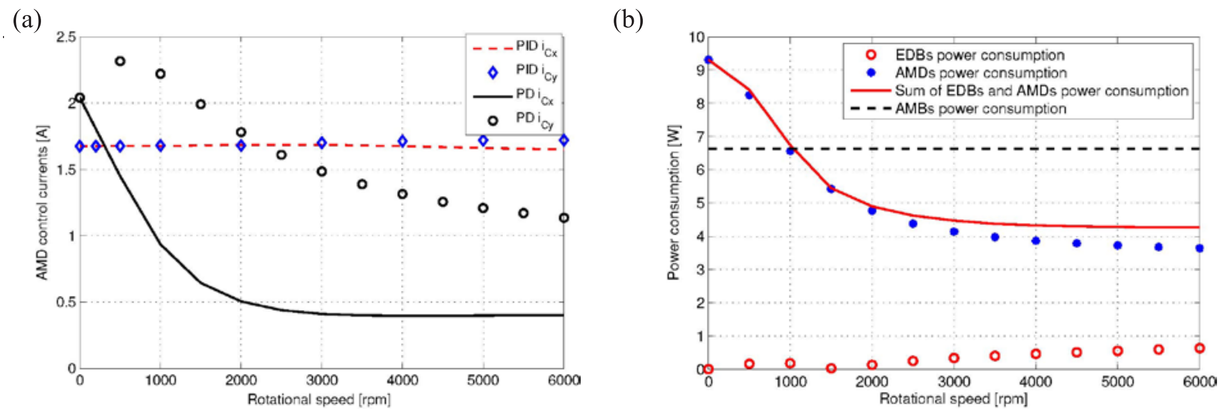

Fig. 8 (a) Control currents according to rotational speed, (b) power consumption in the system.

4. Conclusion

The EDB–AMD system exploits the high reliability of EDBs with the controllability advantage of the AMDs, overcoming limitations of both technologies. In the present paper, a test rig has been built to demonstrate the effectiveness of the proposed hybrid solution. Analytical model of the EDB–AMD system is validated with experimental results. Simulations and experimental tests are exploited for the dynamic characterization of the system. The results have confirmed the effectiveness of the solution. Compared to classical AMBs, the actuator sizes could be reduced and the power consumption is relatively low for high speed operations.

The potential applications are in the fields where the operation speed is high and the required stiffness in relatively low, such as flywheels, centrifuges, small size compressors and vacuum pumps.

References

Amati, N., Lepine, X. DE and Tonoli, A., Modeling of electrodynamic bearings, Journal of Vibration and Acoustics, Vol.130, No.6 (2008), pp.061007.

Amati, N., Detoni, J. G., Impinna, F. and Tonoli, A., Model based design of a rotor supported by radial electrodynamic bearings, 10th International Conference on Vibrations in Rotating Machinery, London, 11-13 September (2012), pp.123-132.

Detoni, J. G., Progress on electrodynamic passive magnetic bearings for rotor levitation, Proceedings of the Institution of Mechanical Engineers. Part C: Journal of Mechanical Engineering Science (2013).

Detoni, J. G., Impinna, F., Amati, N., Tonoli, A., Piccolo, M. P. and Genta, G., Stability of a 4 degree of freedom rotor on electrodynamic passive magnetic bearings, ISMB14, 14th International Symposium on Magnetic Bearings, Linz, Austria, August 11-14 (2014).

Filatov, A., Flywheel Energy Storage System With Homopolar Electrodynamic Magnetic Bearing, Proceedings of the Tenth International Symposium on Magnetic Bearings (2006), Martigny, Switzerland.

Impinna, F., Detoni, J. G., Tonoli, A., Amati, N. and Piccolo, M. P., Test and theory of electrodynamic bearing coupled to active magnetic dampers, ISMB14, 14th International Symposium on Magnetic Bearings, Linz, Austria, August 11-14 (2014).

Schweitzer, G. and Maslen, E., Magnetic Bearings-Theory, Design, and Application on Rotating Machinery (2009), New York, NY, USA: Springer Verlag.

Tonoli, A., Amati, N., Impinna, F. and Detoni, J. G., A solution for the stabilization of electrodynamic bearings: Modeling and experimental validation, Journal of Vibrations and Acoustics, Vol.133, No.021004 (2011), pp.1-10.